New Members of SHG Active Dugganite Family, $A_3BC_3D_2O_{14}$ (A = Ba, Pb; B = Te, Sb; C = Al, Ga, Fe, Zn; D = Si, Ge, P, V): Synthesis, Structure and Materials Properties

Anupam Bhim,[†] Weiguo Zhang,[‡] P. Shiv Halasyamani,*[,‡] Jagannatha Gopalakrishnan*[,†] and Srinivasan Natarajan*[,†]

[†]*Solid State and Structural Chemistry Unit, Indian Institute of Science, Bangalore–560012, India*

[‡]*Department of Chemistry, University of Houston, 112 Fleming Building, Houston, Texas 77204–5003, United States*

Electronic Supporting Information

Table of contents

Table S1. Details of the synthesis conditions for the single phase Dugganite compounds

Compound	Temperature (°C)/Time (h)	Color
$Ba_3TeGa_2ZnSi_2O_{14}$	1075/24	white
$Ba_3TeFe_2ZnSi_2O_{14}$	1060/24	beige
$Pb_3TeGa_2ZnSi_2O_{14}$	720/24	white
$Pb_3TeFe_2ZnSi_2O_{14}$	710/24	beige
$Pb_3TeAl_2ZnSi_2O_{14}$	730/24	white
$Pb_3TeGa_2ZnGe_2O_{14}$	710/24	white
$Pb_3TeFe_2ZnGe_2O_{14}$	700/24	yellow
$Pb_3SbGaZn_2P_2O_{14}$	800/24	white
$Pb_3SbFeZn_2P_2O_{14}$	790/24	yellowish
$PbBa_2TeZn_3V_2O_{14}$	870/48	white
$Pb_2BaTeZn_3V_2O_{14}$	780/48	white

(a)

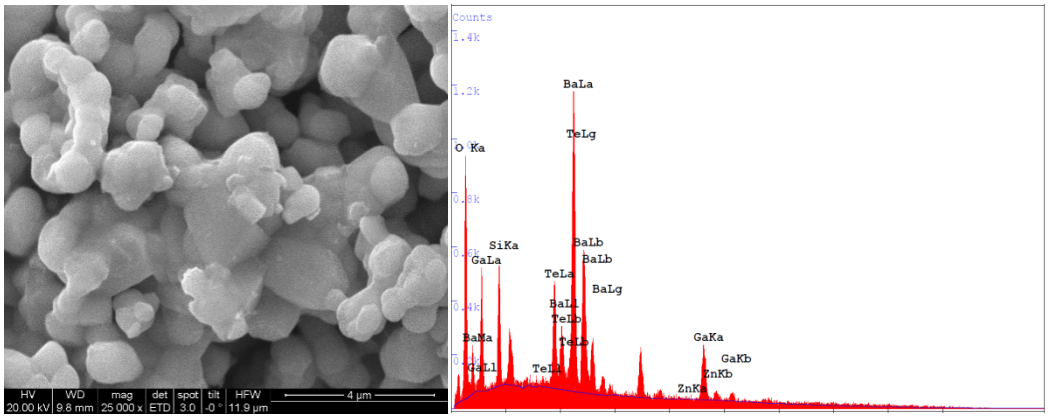
HV 20.00 kV | WD 9.8 mm | mag 25 000 x | det ETD | spot 3.0 | tilt -0 ° | HFW 11.9 µm | 4 µm
Counts
BaLa
TeLg
O Ka
SiKa
GaLa
BaLb
TeLa
BaLg
BaLl
TeLb
BaMa
GaKa
GaKb
ZnKb
GaLl
TeLl
ZnKa
2.00
4.00
6.00
8.00
10.00
12.00
keV

(b)

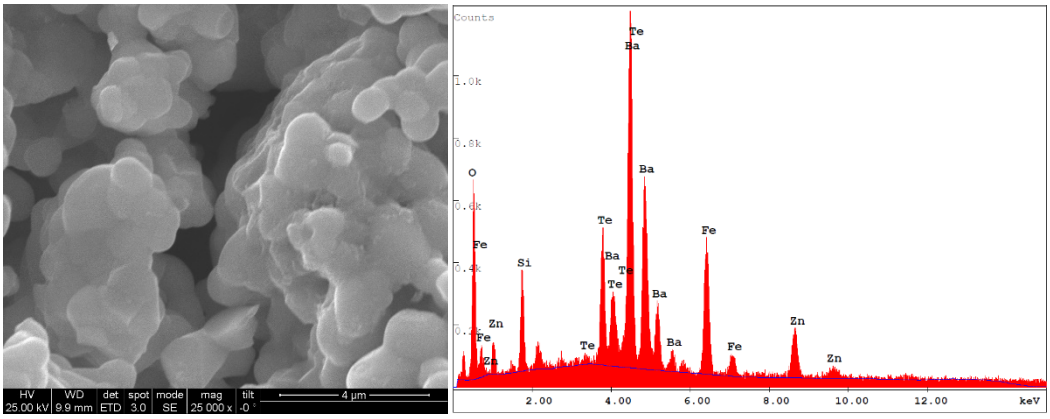
HV 25.00 kV | WD 9.9 mm | det ETD | spot 3.0 | mode SE | mag 25 000 x | tilt -0 ° | 4 µm
Counts
Te
Ba
O
Fe
Si
Zn
2.00
4.00
6.00
8.00
10.00
12.00
keV

(c)

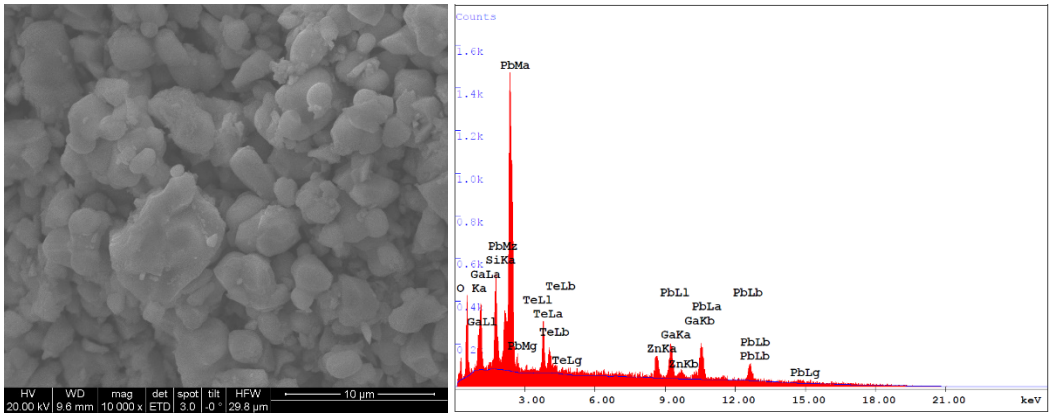
HV 20.00 kV | WD 9.6 mm | mag 10 000 x | det ETD | spot 3.0 | tilt -0 ° | HFW 29.8 µm | 10 µm
Counts
PbMa
PbMz
SiKa
GaLa
O Ka
TeLb
TeLl
TeLa
GaLl
PbMg
TeLg
PbLl
PbLb
PbLa
GaKb
GaKa
ZnKa
ZnKb
3.00
6.00
9.00
12.00
15.00
18.00
21.00
keV

(d)

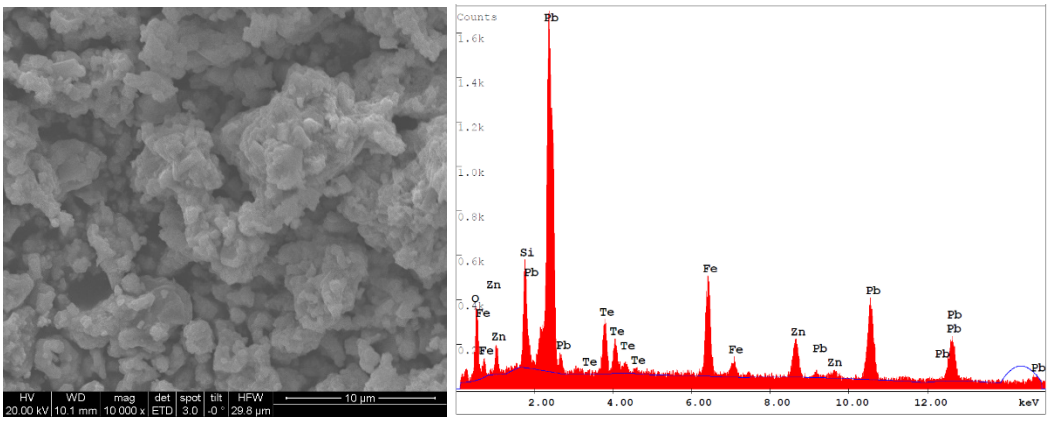
HV 20.00 kV | WD 10.1 mm | mag 10 000 x | det ETD | spot 3.0 | tilt -0 ° | HFW 29.8 µm | 10 µm
Counts
Pb
Si
Zn
O
Fe
Te
2.00
4.00
6.00
8.00
10.00
12.00
keV

(e)

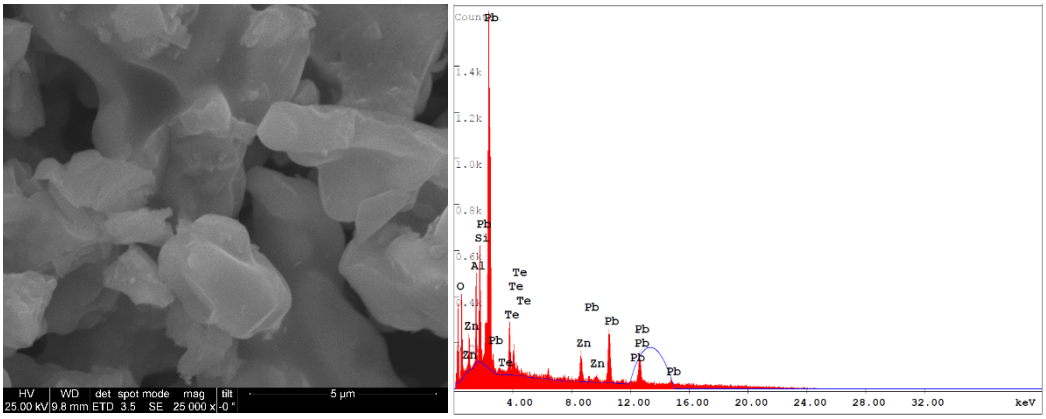
HV WD det spot mode mag tilt
25.00 kV 9.8 mm ETD 3.5 SE 25 000 x -0 °
5 µm
Counts
Pb
Si
Al
O
Te
Zn
Ga
4.00 8.00 12.00 16.00 20.00 24.00 28.00 32.00 keV

(f)

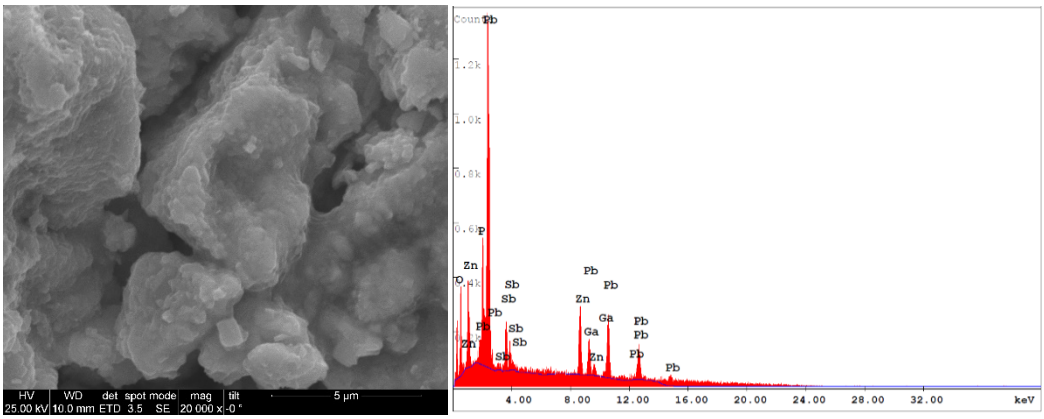
HV WD det spot mode mag tilt
25.00 kV 10.0 mm ETD 3.5 SE 20 000 x -0 °
5 µm
Counts
Pb
Zn
O
Sb
Ga
4.00 8.00 12.00 16.00 20.00 24.00 28.00 32.00 keV

(g)

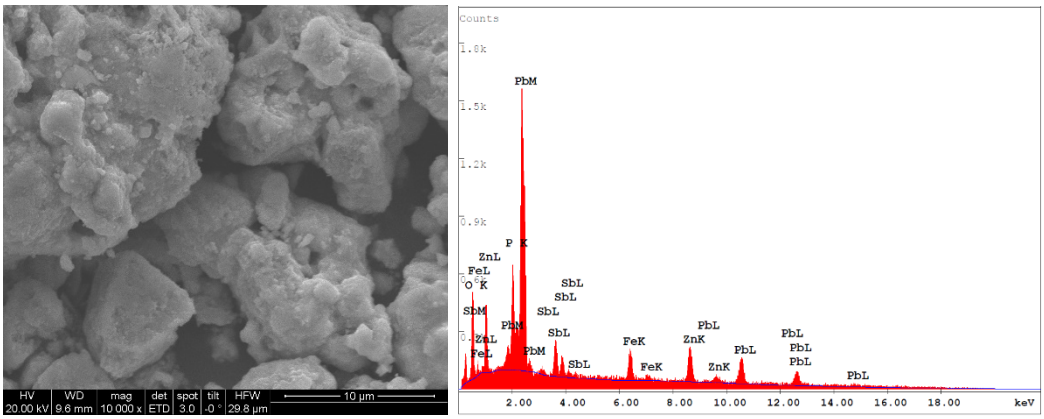
HV WD mag det spot tilt HFW
20.00 kV 9.6 mm 10 000 x ETD 3.0 -0 ° 29.8 µm
10 µm
Counts
PbM
ZnL
FeL
O K
SbM
SbL
PbL
ZnK
FeK
2.00 4.00 6.00 8.00 10.00 12.00 14.00 16.00 18.00 keV

(h)

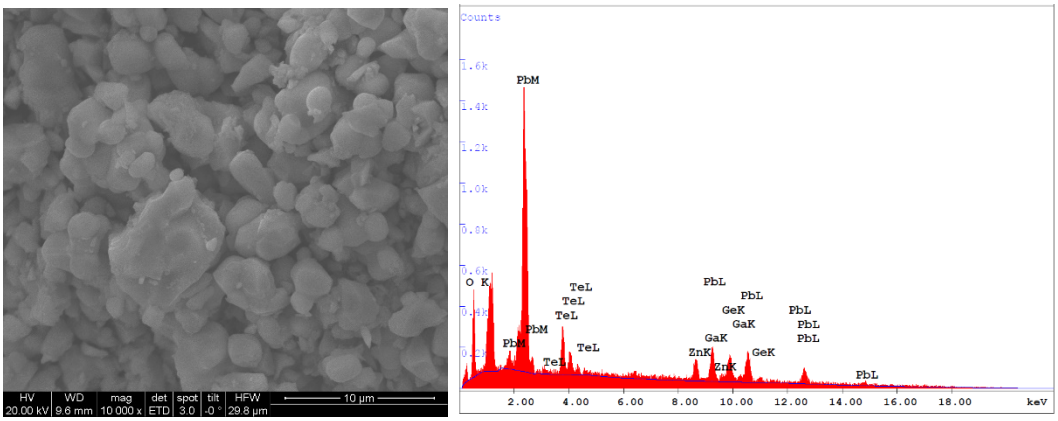
HV WD mag det spot tilt HFW
20.00 kV 9.6 mm 10 000 x ETD 3.0 -0 ° 29.8 µm
10 µm
Counts
PbM
O K
TeL
PbL
GeK
GaK
ZnK
2.00 4.00 6.00 8.00 10.00 12.00 14.00 16.00 18.00 keV

(i)

(j)

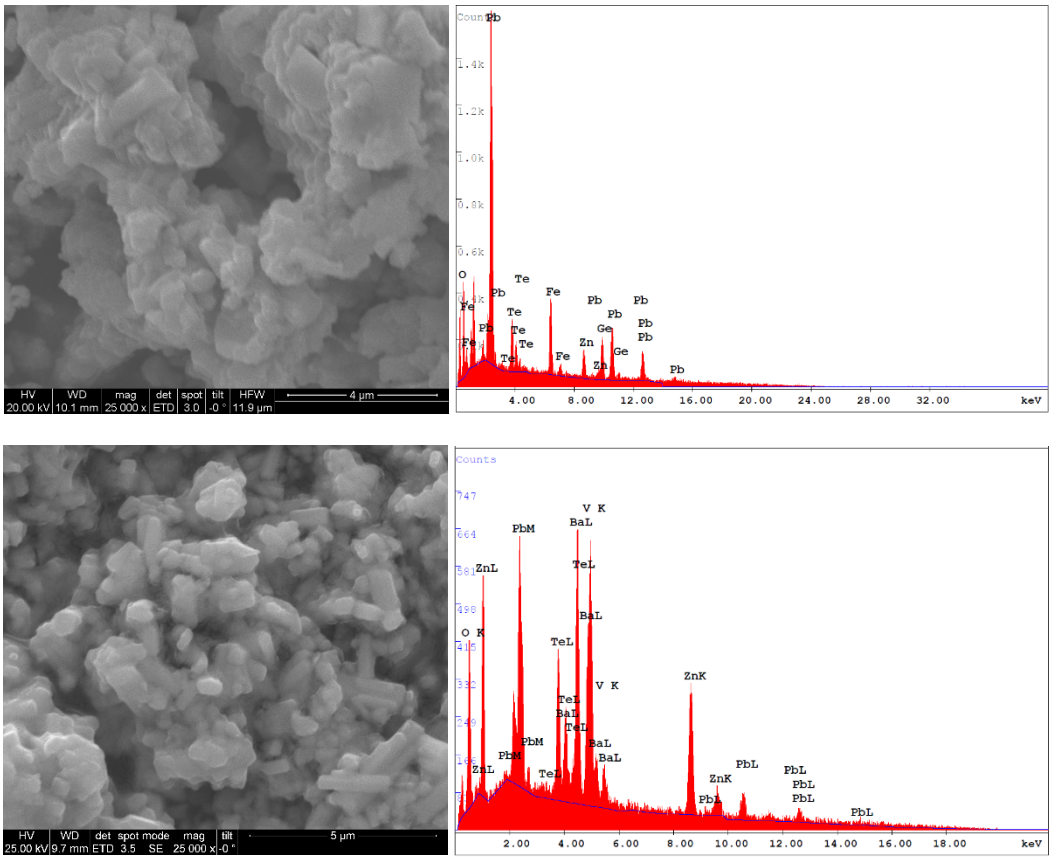

Figure S1. SEM image and corresponding EDX spectrum of (a) $Ba_3TeGa_2ZnSi_2O_{14}$ (b) $Ba_3TeFe_2ZnSi_2O_{14}$ (c) $Pb_3TeGa_2ZnSi_2O_{14}$ (d) $Pb_3TeFe_2ZnSi_2O_{14}$ (e) $Pb_3TeAl_2ZnSi_2O_{14}$ (f) $Pb_3SbGaZn_2P_2O_{14}$ (g) $Pb_3SbFeZn_2P_2O_{14}$ (h) $Pb_3TeGa_2ZnGe_2O_{14}$ (i) $Pb_3TeFe_2ZnGe_2O_{14}$ (j) $PbBa_2TeZn_3V_2O_{14}$

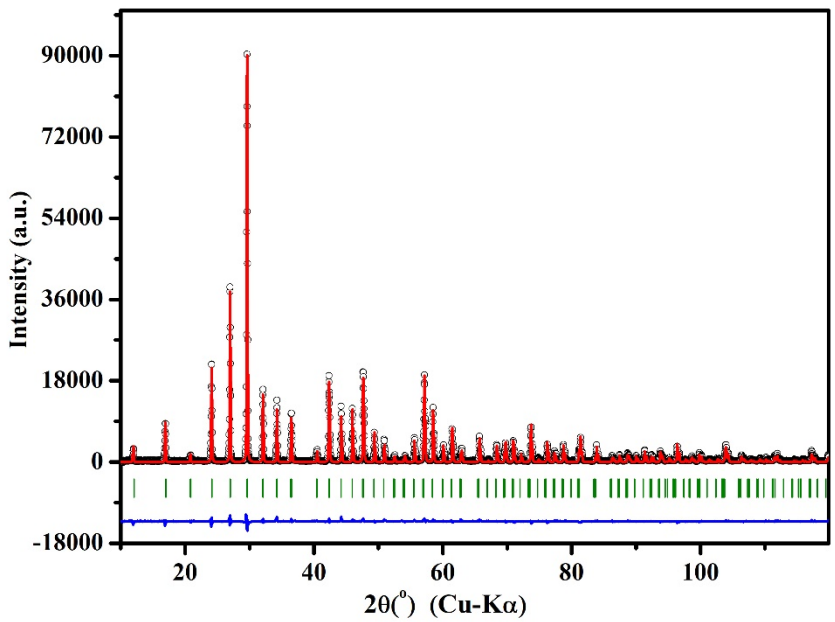

Figure S2. Rietveld refinement of $Ba_3TeFe_2ZnSi_2O_{14}$ from the PXRD data. The observed (O), calculated (red line), and difference (bottom blue line) profiles are shown. The vertical bars (|) indicate Bragg reflections.

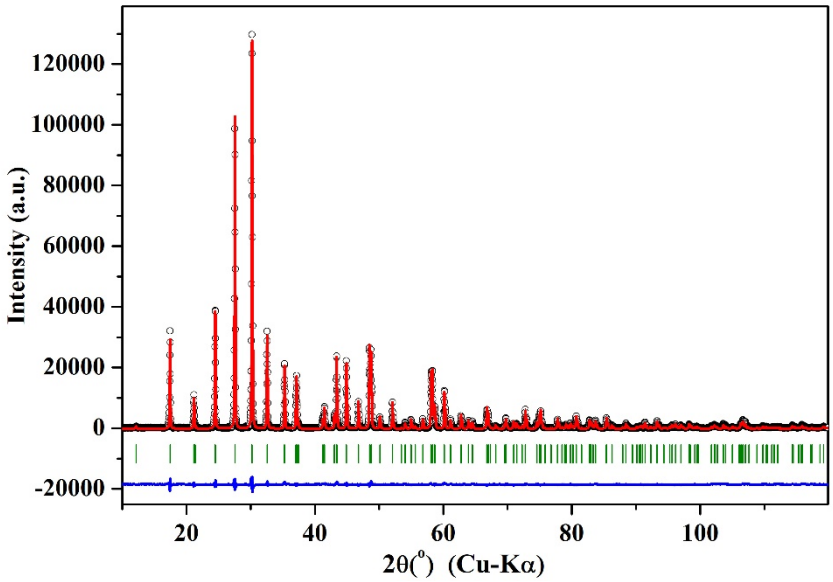

Figure S3. Rietveld refinement of $Pb_3TeGa_2ZnSi_2O_{14}$ from the PXRD data. The observed (O), calculated (red line), and difference (bottom blue line) profiles are shown. The vertical bars (|) indicate Bragg reflections.

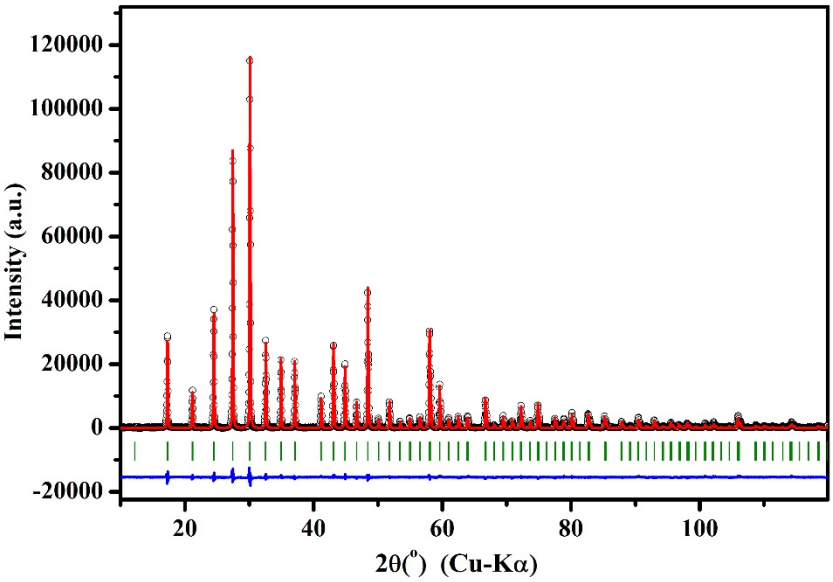

Figure S4. Rietveld refinement of $Pb_3TeFe_2ZnSi_2O_{14}$ from the PXRD data. The observed (O), calculated (red line), and difference (bottom blue line) profiles are shown. The vertical bars (|) indicate Bragg reflections.

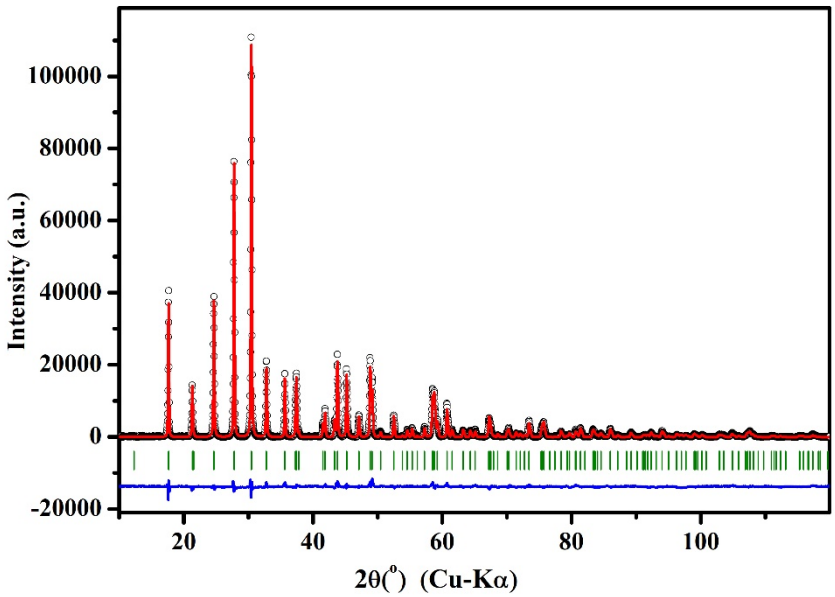

Figure S5. Rietveld refinement of $Pb_3TeAl_2ZnSi_2O_{14}$ from the PXRD data. The observed (O), calculated (red line), and difference (bottom blue line) profiles are shown. The vertical bars (|) indicate Bragg reflections.

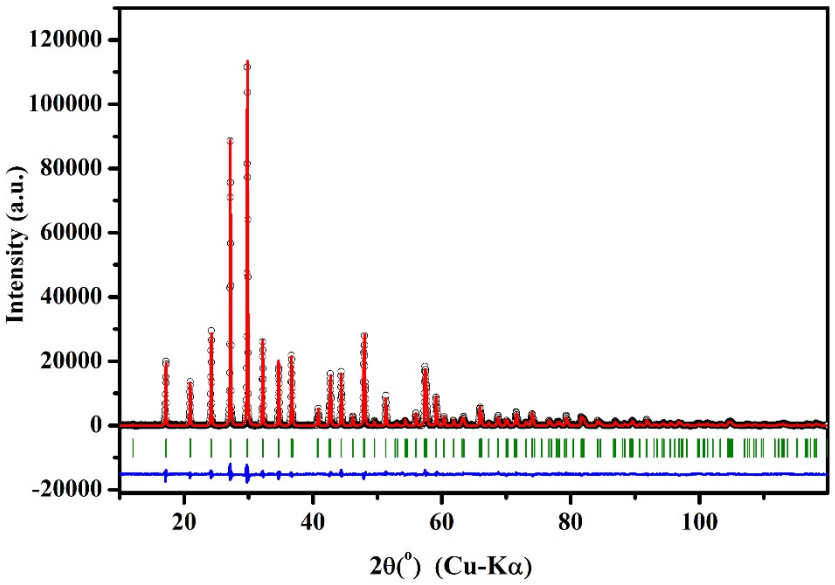

Figure S6. Rietveld refinement of $Pb_3TeFe_2ZnGe_2O_{14}$ from the PXRD data. The observed (O), calculated (red line), and difference (bottom blue line) profiles are shown. The vertical bars (|) indicate Bragg reflections.

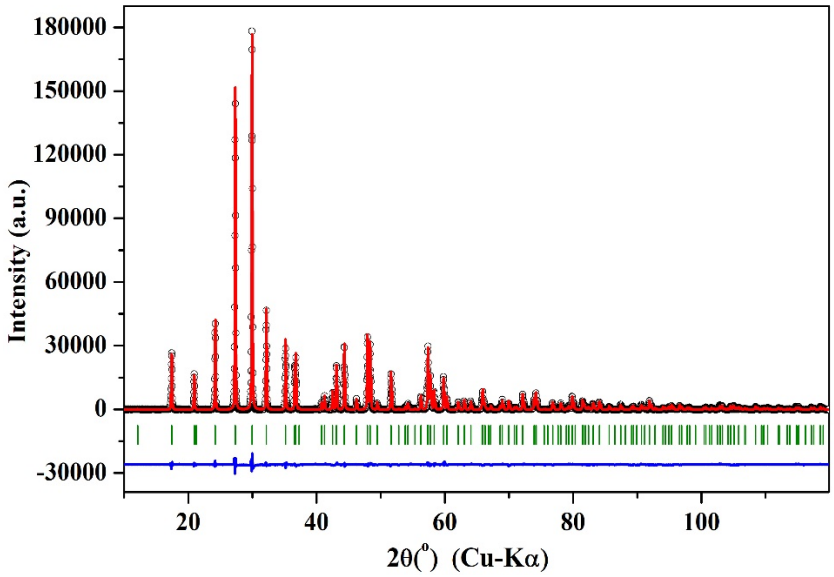

Figure S7. Rietveld refinement of $Pb_3TeGa_2ZnGe_2O_{14}$ from the PXRD data. The observed (O), calculated (red line), and difference (bottom blue line) profiles are shown. The vertical bars (|) indicate Bragg reflections.

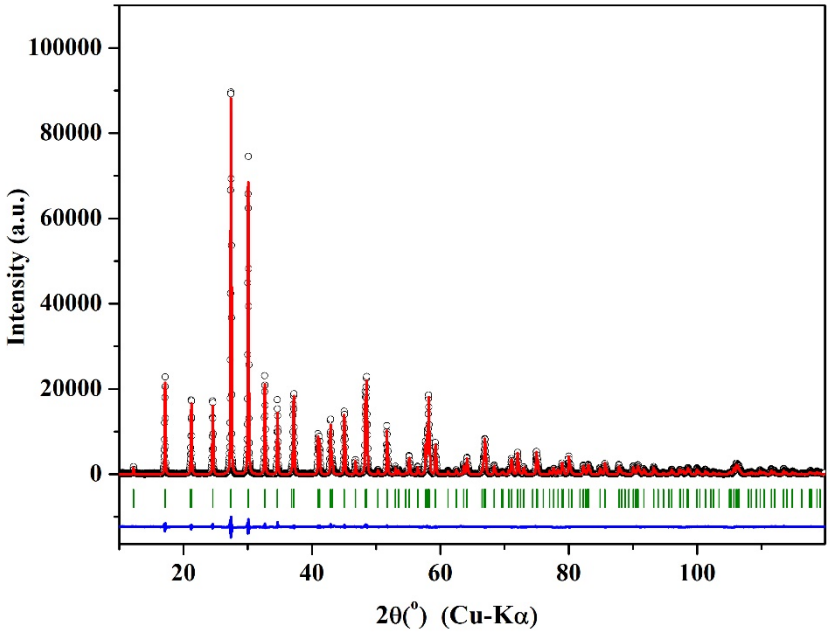

Figure S8. Rietveld refinement of $Pb_3SbGaZn_2P_2O_{14}$ from the PXRD data. The observed (O), calculated (red line), and difference (bottom blue line) profiles are shown. The vertical bars (|) indicate Bragg reflections.

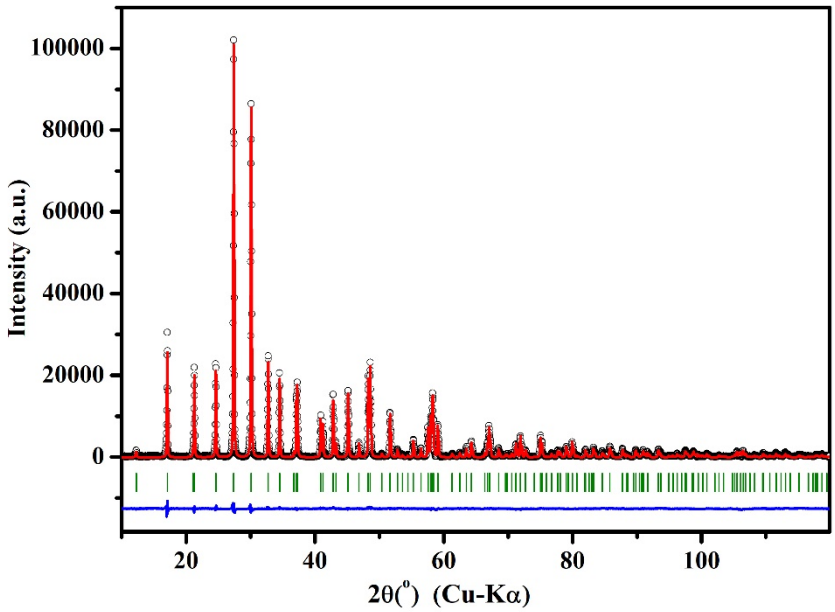

Figure S9. Rietveld refinement of $Pb_3SbFeZn_2P_2O_{14}$ from the PXRD data. The observed (O), calculated (red line), and difference (bottom blue line) profiles are shown. The vertical bars (|) indicate Bragg reflections.

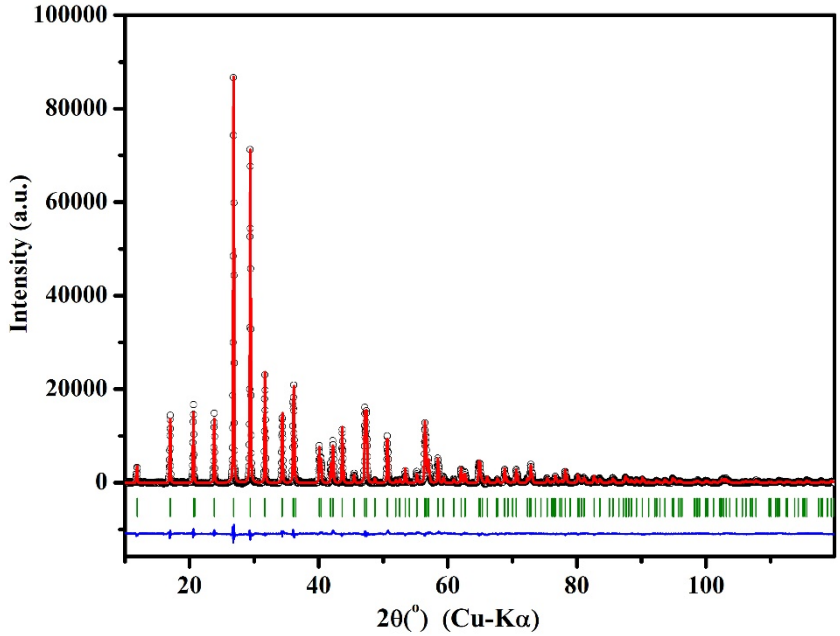

Figure S10. Rietveld refinement of $Pb_2BaTeZn_3V_2O_{14}$ from the PXRD data. The observed (O), calculated (red line), and difference (bottom blue line) profiles are shown. The vertical bars (|) indicate Bragg reflections.

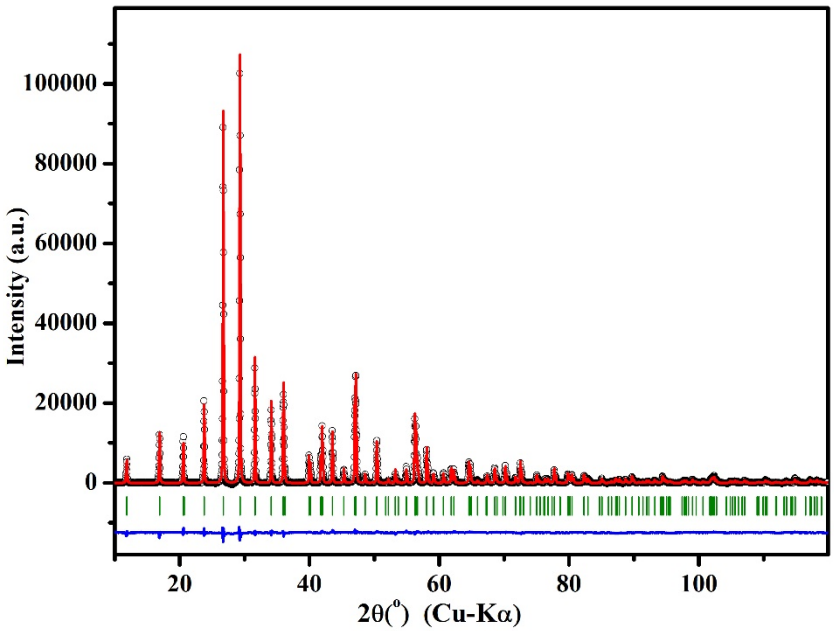

Figure S11. Rietveld refinement of $PbBa_2TeZn_3V_2O_{14}$ from the PXRD data. The observed (O), calculated (red line), and difference (bottom blue line) profiles are shown. The vertical bars (|) indicate Bragg reflections.

Table S2. Crystallographic data for $Ba_3TeFe_2ZnSi_2O_{14}$.

Atom	Site	x	y	z	U_{iso}(Å^2)	Occupancy
Ba	*3e*	0.442(3)	0.0	0.0	0.010(1)	1.0
Te	*1a*	0.0	0.0	0.0	0.013(2)	1.0
Fe/Zn	*3f*	0.756(4)	0.0	0.5	0.003(2)	0.666/0.334
Si	*2d*	0.333	0.667	0.472(3)	0.003(4)	1.0
O1	*2d*	0.333	0.667	0.763(2)	0.009(1)	1.0
O2	*6g*	0.492(3)	0.300(2)	0.637(2)	0.002(1)	1.0
O3	*6g*	0.220(9)	0.102(2)	0.228(4)	0.032(3)	1.0

Space group *P*321: $a = b$ = 8.520(1) Å, c = 5.234 (1) Å, $\alpha = \beta = 90°$, $\gamma = 120°$;

Reliability Factors: R_p = 2.23%, R_{wp} = 3.24%, χ^2 = 4.52;

Bond Lengths (Å):

Fe/Zn–O = 1.931(1), Te–O = 2.02(1), Si–O = 1.494(2),

Ba–O = 2.825 (average)

Table S3. Crystallographic data for $Pb_3TeGa_2ZnSi_2O_{14}$.

Atom	Site	x	y	z	U_{iso}(Å^2)	Occupancy
Pb	*3e*	0.426(3)	0.426(3)	1.0	0.033(2)	1.0
Te	*1a*	0.0	0.0	1.0	0.021(4)	1.0
Ga/Zn	*3f*	0.254(3)	0.0	0.5	0.018(2)	0.666/0.334
Si	*2d*	0.333	0.667	0.529(2)	0.009(1)	1.0
O1	*2d*	0.333	0.667	0.220(5)	0.009(2)	1.0
O2	*6g*	0.221(8)	0.123(3)	0.767(1)	0.021(5)	1.0
O3	*6g*	0.189(4)	0.497(2)	0.652(6)	0.038(1)	1.0

Space group *P*321: $a = b$ = 8.405(1) Å, c = 5.090 (1) Å, $\alpha = \beta$ = 90°, γ =120°;

Reliability Factors: R_p = 3.51%, R_{wp} = 4.57%, χ^2 = 2.38;

Bond Lengths (Å):

Ga/Zn–O = 1.901(1), Te–O = 2.002(1), Si–O = 1.497(2),

Pb–O = 2.741 (average)

Table S4. Crystallographic data for $Pb_3TeFe_2ZnSi_2O_{14}$.

Atom	Site	x	y	z	U_{iso}(Å^2)	Occupancy
Pb	*3e*	0.425(4)	0.425(4)	1.0	0.032(5)	1.0
Te	*1a*	0.0	0.0	1.0	0.025(2)	1.0
Fe/Zn	*3f*	0.252(1)	0.0	0.5	0.021(6)	0.666/0.334
Si	*2d*	0.333	0.667	0.508(4)	0.009(1)	1.0
O1	*2d*	0.333	0.667	0.210(3)	0.006(1)	1.0
O2	*6g*	0.220(9)	0.120(4)	0.763(10)	0.038(7)	1.0
O3	*6g*	0.185(5)	0.499(1)	0.640(2)	0.063(4)	1.0

Space group *P*321: $a = b$ = 8.419(1) Å, c = 5.146 (1) Å, $\alpha = \beta$ = 90°, γ =120°;

Reliability Factors: R_p = 2.11%, R_{wp} = 3.18%, χ^2 = 6.25;

Bond Lengths (Å):

Fe/Zn–O = 1.909(1), Te–O = 2.018(1), Si–O = 1.507(2),

Pb–O = 2.755 (average)

Table S5. Crystallographic data for $Pb_3TeAl_2ZnSi_2O_{14}$.

Atom	Site	x	y	z	U_{iso}(Å^2)	Occupancy
Pb	*3e*	0.425(7)	0.425(7)	1.0	0.032(6)	1.0
Te	*1a*	0.0	0.0	1.0	0.020(1)	1.0
Al/Zn	*3f*	0.259(5)	0.0	0.5	0.013(7)	0.666/0.334
Si	*2d*	0.333	0.667	0.529(1)	0.012(4)	1.0
O1	*2d*	0.333	0.667	0.232(3)	0.011(6)	1.0
O2	*6g*	0.221(4)	0.120(4)	0.768(2)	0.001(5)	1.0
O3	*6g*	0.192(3)	0.475(8)	0.632(9)	0.068(3)	1.0

Space group *P*321: $a = b$ = 8.365(1) Å, c = 5.93(1) Å, $\alpha = \beta = 90°$, $\gamma = 120°$;

Reliability Factors: R_p = 3.17%, R_{wp} = 3.83%, χ^2 = 6.45;

Bond Lengths (Å):

Al/Zn–O = 1.887(1), Te–O = 1.991(2), Si–O = 1.52(2),

Pb–O = 2.749(average)

Table S6. Crystallographic data for $Pb_3TeFe_2ZnGe_2O_{14}$.

Atom	Site	x	y	z	U_{iso}(Å^2)	Occupancy
Pb	*3e*	0.423(2)	0.423(2)	1.0	0.037(2)	1.0
Te	*1a*	0.0	0.0	1.0	0.026(9)	1.0
Fe/Zn	*3f*	0.242(1)	0.0	0.5	0.027(4)	0.666/0.334
Ge	*2d*	0.333	0.667	0.514(2)	0.024(4)	1.0
O1	*2d*	0.333	0.667	0.195(5)	0.022(2)	1.0
O2	*6g*	0.214(2)	0.120(9)	0.783(7)	0.016(8)	1.0
O3	*6g*	0.172(8)	0.497(12)	0.650(3)	0.066(1)	1.0

Space group *P*321: $a = b$ = 8.502(1) Å, c = 5.177(1) Å, $\alpha = \beta = 90°$, $\gamma = 120°$;

Reliability Factors: R_p = 2.31%, R_{wp} = 2.42%, χ^2 = 4.12;

Bond Lengths (Å):

Fe/Zn–O = 1.921(1), Te–O = 1.981(2), Ge–O = 1.56(1),

Pb–O = 2.742 (average)

Table S7. Crystallographic data for $Pb_3TeGa_2ZnGe_2O_{14}$.

Atom	Site	x	y	z	U_{iso}(Å^2)	Occupancy
Pb	*3e*	0.422(7)	0.422(7)	1.0	0.037(5)	1.0
Te	*1a*	0.0	0.0	1.0	0.022(4)	1.0
Ga/Zn	*3f*	0.250(3)	0.0	0.5	0.017(1)	0.666/0.334
Ge	*2d*	0.333	0.667	0.476(8)	0.021(4)	1.0
O1	*2d*	0.333	0.667	0.208(3)	0.091(11)	1.0
O2	*6g*	0.215(2)	0.121(9)	0.771(4)	0.019(2)	1.0
O3	*6g*	0.175(4)	0.459(11)	0.668(7)	0.041(1)	1.0

Space group *P*321: $a = b$ = 8.523(1) Å, c = 5.116(1) Å, $\alpha = \beta$ = 90°, γ =120°;

Reliability Factors: R_p = 3.26%, R_{wp} = 4.64%, χ^2 = 4.782;

Bond Lengths (Å):

Ga/Zn–O = 1.919(1), Te–O = 1.978(1), Ge–O = 1.57(2),

Pb–O = 2.744(average)

Table S8. Crystallographic data for $Pb_3SbGaZn_2P_2O_{14}$.

Atom	Site	x	y	z	U_{iso}(Å^2)	Occupancy
Pb	*3e*	0.406(2)	0.406(2)	1.0	0.022(8)	1.0
Sb	*1a*	0.0	0.0	1.0	0.015(2)	1.0
Ga/Zn	*3f*	0.247(6)	0.0	0.5	0.021(9)	0.666/0.334
P	*2d*	0.333	0.667	0.544(2)	0.017(6)	1.0
O1	*2d*	0.333	0.667	0.234(7)	0.034(3)	1.0
O2	*6g*	0.206(8)	0.121(6)	0.756(3)	0.067(2)	1.0
O3	*6g*	0.199(7)	0.485(7)	0.652(2)	0.032(3)	1.0

Space group *P*321: $a = b$ = 8.379(2) Å, c = 5.182(1) Å, $\alpha = \beta$ = 90°, γ =120°;

Reliability Factors: R_p = 2.61%, R_{wp} = 3.62%, χ^2 = 6.197;

Bond Lengths (Å):

Ga/Zn–O = 1.911(3), Sb–O = 1.969(1), P–O = 1.505(1),

Pb–O = 2.741(average)

Table S9. Crystallographic data for $Pb_3SbFeZn_2P_2O_{14}$.

Atom	Site	x	y	z	U_{iso}(Å^2)	Occupancy
Pb	*3e*	0.408(7)	0.408(7)	1.0	0.029(4)	1.0
Sb	*1a*	0.0	0.0	1.0	0.026(3)	1.0
Fe/Zn	*3f*	0.247(1)	0.0	0.5	0.027(2)	0.666/0.334
P	*2d*	0.333	0.667	0.545(4)	0.008(1)	1.0
O1	*2d*	0.333	0.667	0.232(3)	0.057(7)	1.0
O2	*6g*	0.207(5)	0.121(8)	0.752(6)	0.055(9)	1.0
O3	*6g*	0.198(12)	0.488(7)	0.660(4)	0.058(2)	1.0

Space group *P*321: $a = b$ = 8.366(2) Å, c = 5.202(1) Å, $\alpha = \beta = 90°$, $\gamma = 120°$;

Reliability Factors: R_p = 2.24%, R_{wp} = 3.02%, χ^2 = 5.423;

Bond Lengths (Å):

Fe/Zn–O = 1.916(2), Sb–O = 1.984(1), P–O = 1.512(2),

Pb–O = 2.737(average)

Table S10. Crystallographic data for $Pb_2BaTeZn_3V_2O_{14}$.

Atom	Site	x	y	z	U_{iso}(Å^2)	Occupancy
Pb/Ba	*3e*	0.405(4)	0.405(4)	1.0	0.040(7)	0.666/0.334
Te	*1a*	0.0	0.0	1.0	0.032(8)	1.0
Zn	*3f*	0.0	0.237(8)	0.5	0.027(2)	1.0
V	*2d*	0.667	0.333	0.511(9)	0.020(6)	1.0
O1	*2d*	0.667	0.333	0.209(4)	0.024(4)	1.0
O2	*6g*	0.127(4)	0.210(8)	0.777(5)	0.107(1)	1.0
O3	*6g*	0.461(7)	0.191(2)	0.670(6)	0.035(3)	1.0

Space group *P*321: $a = b$ = 8.634(2) Å, c = 5.224(1) Å, $\alpha = \beta = 90°$, $\gamma = 120°$;

Reliability Factors: R_p = 2.50%, R_{wp} = 3.38%, χ^2 = 5.709;

Bond Lengths (Å):

Zn–O = 1.974(2), Te–O = 1.968(1), V–O = 1.702(1),

Pb/Ba–O = 2.747(average)

Table S11. Crystallographic data for $PbBa_2TeZn_3V_2O_{14}$.

Atom	Site	x	y	z	$U_{iso}(Å^2)$	Occupancy
Pb/Ba	*3e*	0.394(8)	0.394(8)	1.0	0.035(3)	0.334/0.666
Te	*1a*	0.0	0.0	1.0	0.023(2)	1.0
Zn	*3f*	0.0	0.230(4)	0.5	0.023(8)	1.0
V	*2d*	0.667	0.333	0.530(11)	0.024(7)	1.0
O1	*2d*	0.667	0.333	0.222(7)	0.083(4)	1.0
O2	*6g*	0.124(2)	0.212(6)	0.780(3)	0.067(9)	1.0
O3	*6g*	0.468(6)	0.189(5)	0.668(4)	0.040(1)	1.0

Space group *P*321: $a = b = 8.664(2)$ Å, $c = 5.262(1)$ Å, $\alpha = \beta = 90°$, $\gamma = 120°$;

Reliability Factors: $R_p = 2.28\%$, $R_{wp} = 3.68\%$, $\chi^2 = 3.123$;

Bond Lengths (Å):

Zn–O = 1.981(2), Te–O = 1.975(1), V–O = 1.691(2),

Pb/Ba–O = 2.769(average)

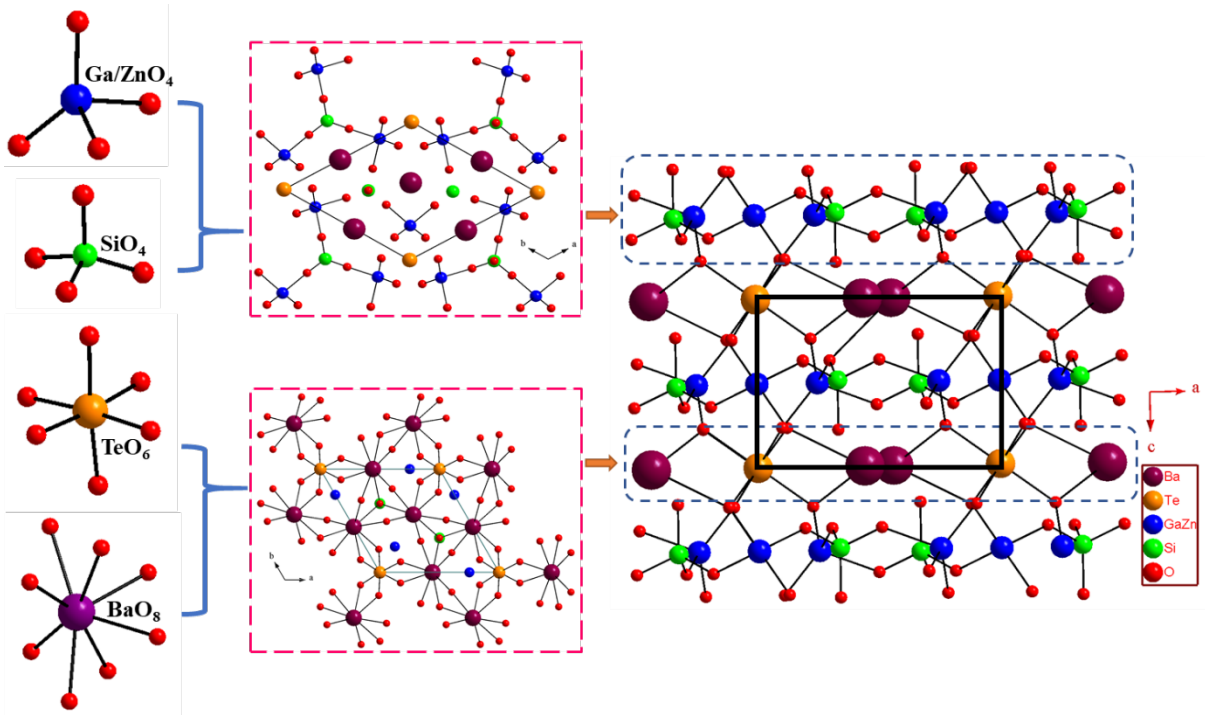

Figure S12. Crystal structure of $Ba_3TeGa_2ZnSi_2O_{14}$

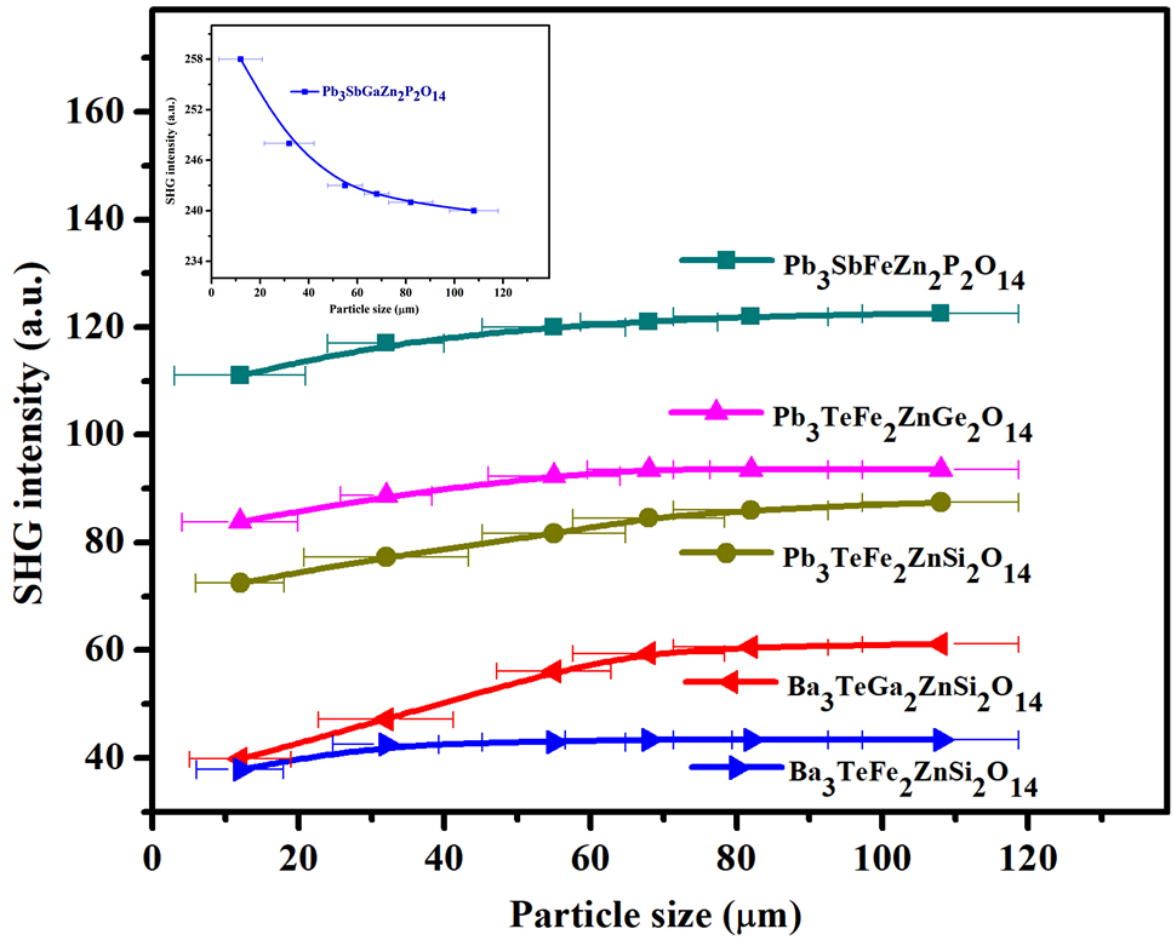

Figure S13. Phase-matching data for moderate phase-matchable SHG active new Dugganite compounds. Inset showing non-phase-matchable SHG active compound, $Pb_3SbGaZn_2P_2O_{14}$. The solid curves are drawn to guide the eye and are not a fit to the data.

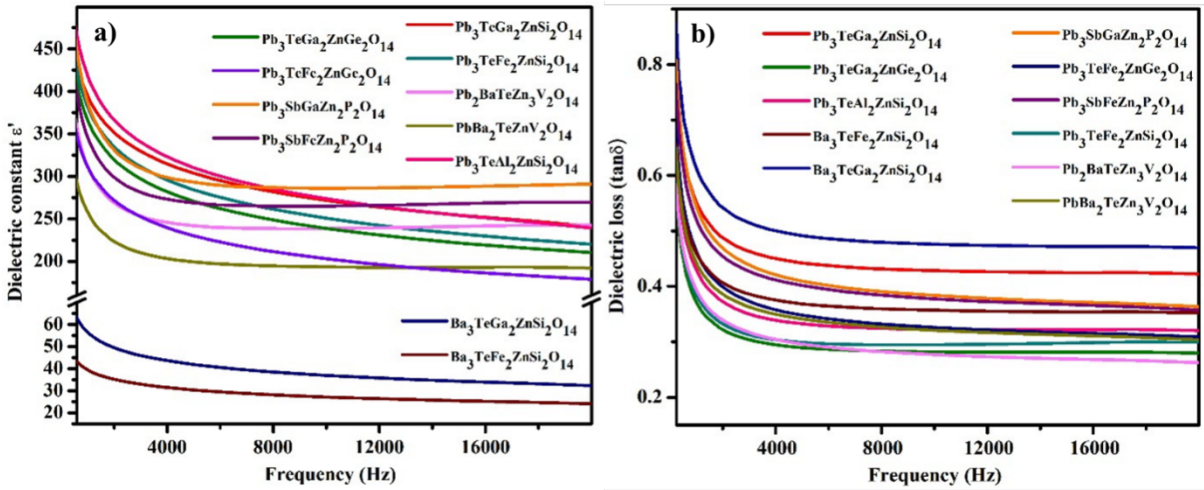

Figure S14. (a)The dielectric constant and (b) dielectric loss versus frequency plots for all Dugganites at room temperature.

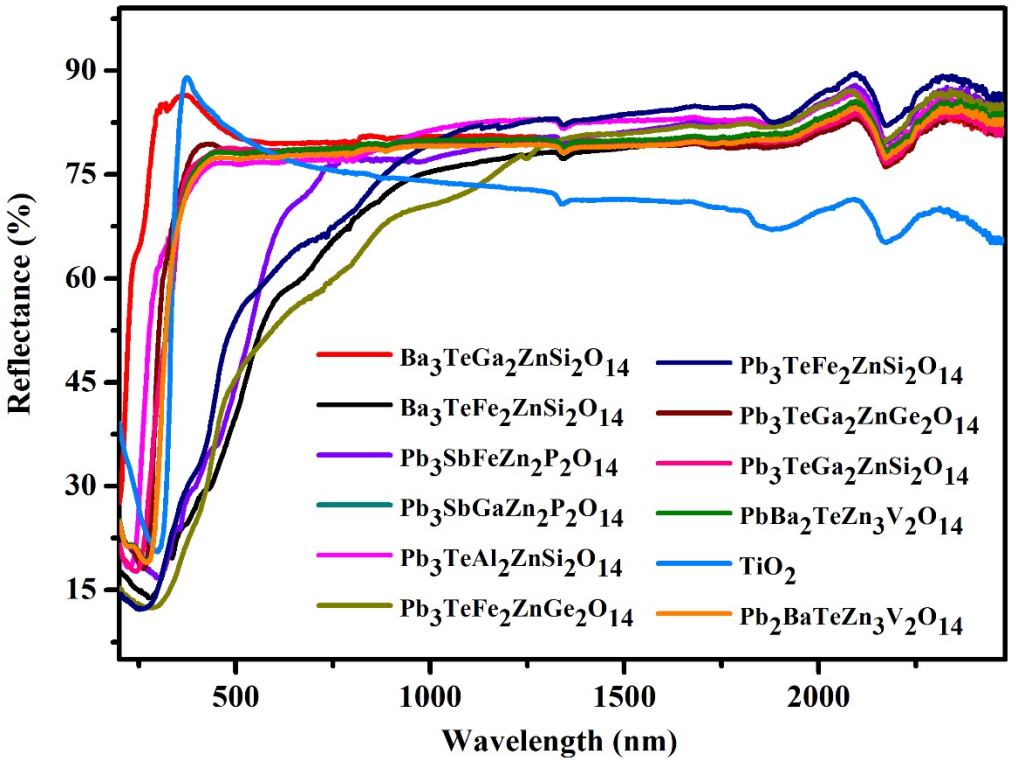

Figure S15. Comparison of UV/Vis and NIR reflectance (%) of dugganite compounds with TiO_2.

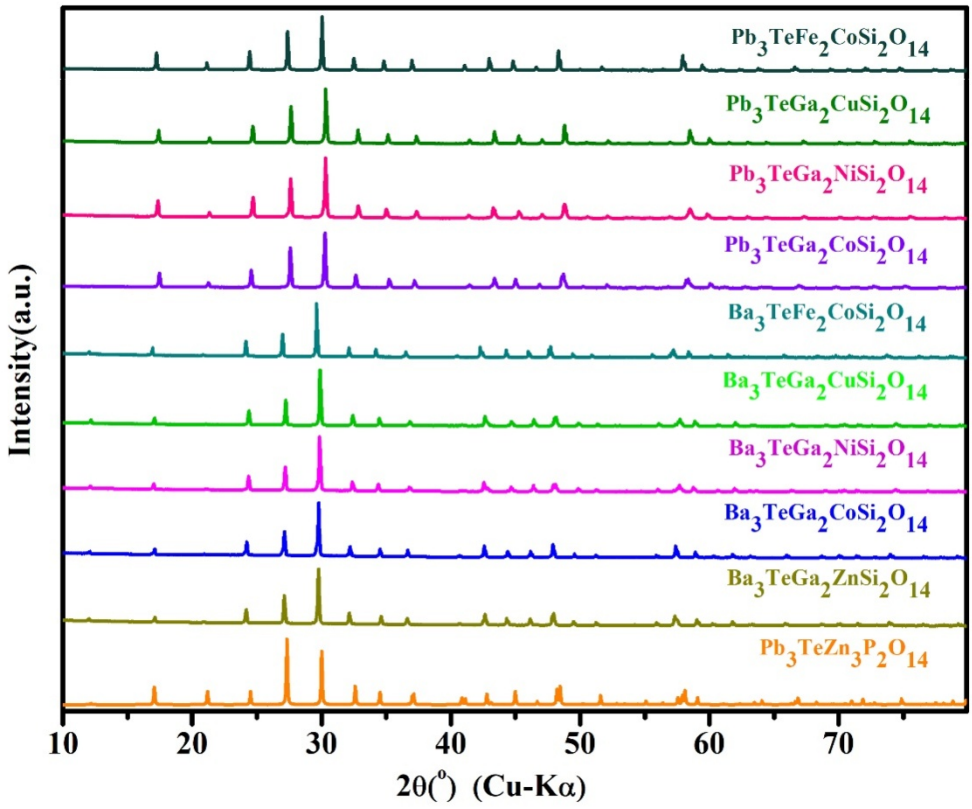

Figure S16. PXRD patterns of different $(Ba/Pb)_3Te(Ga/Fe)_2ZnM^{II}Si_2O_{14}$ (M^{II}=Co, Ni, and Cu)

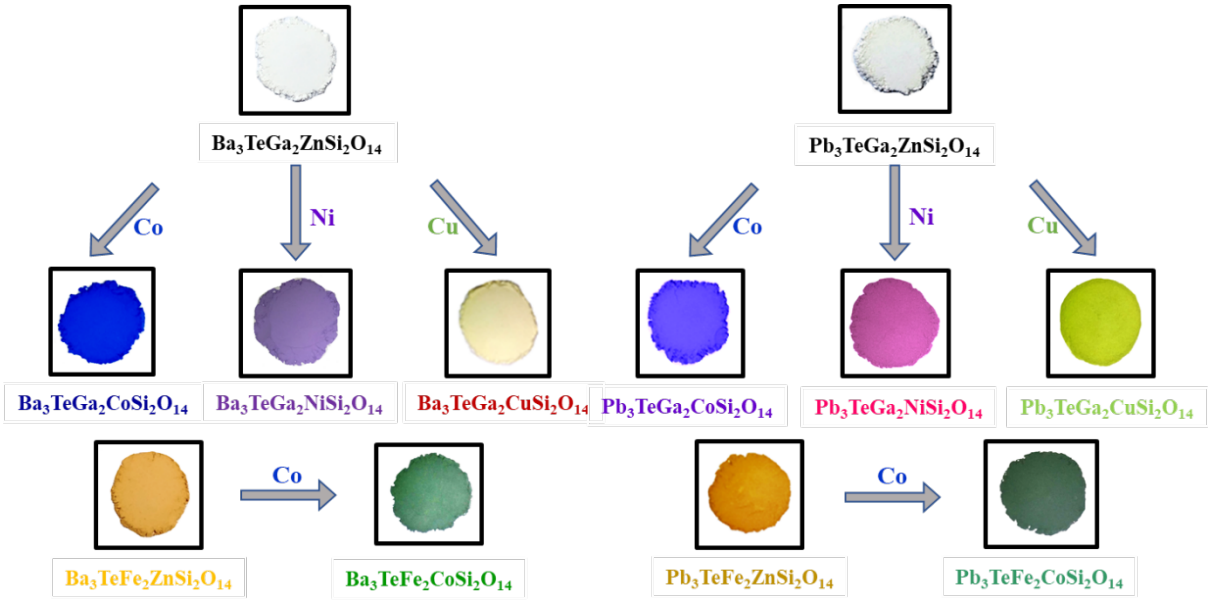

Figure S17. Colors of $(Ba/Pb)_3TeGa_2ZnM^{II}Si_2O_{14}$ (M^{II}=Co, Ni, and Cu) under daylight

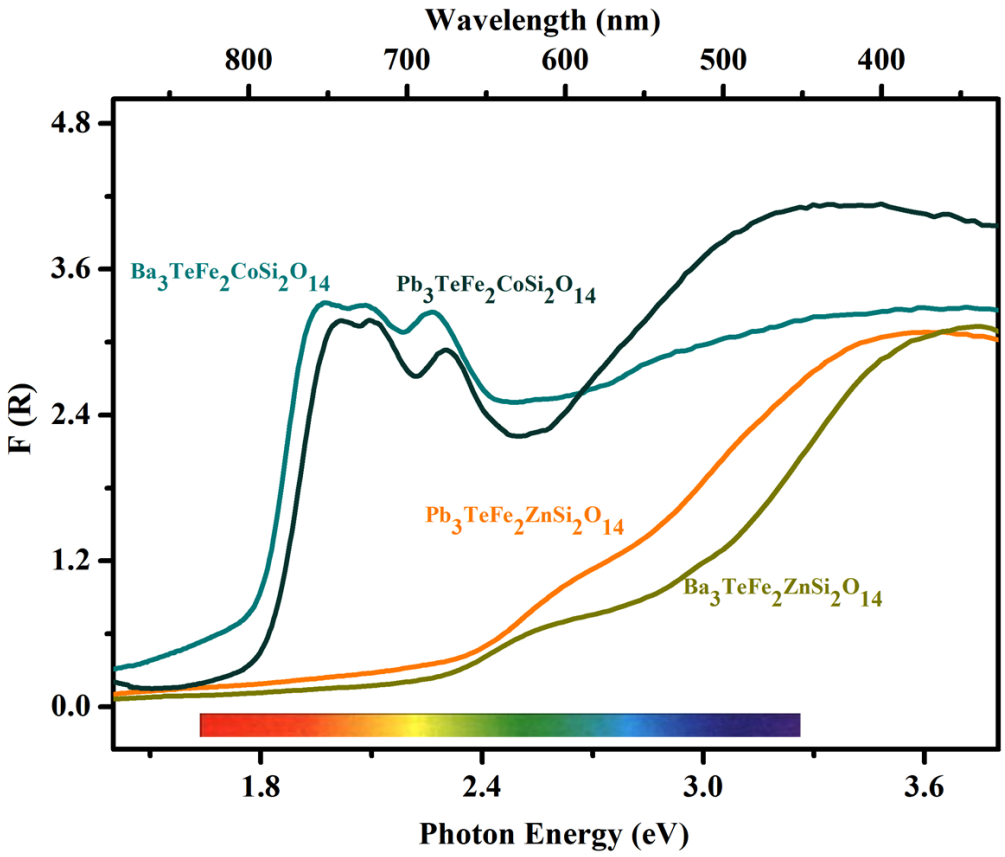

Figure S18. Optical absorption (UV/Vis) spectra of $(Ba/Pb)_3TeFe_2CoSi_2O_{14}$.

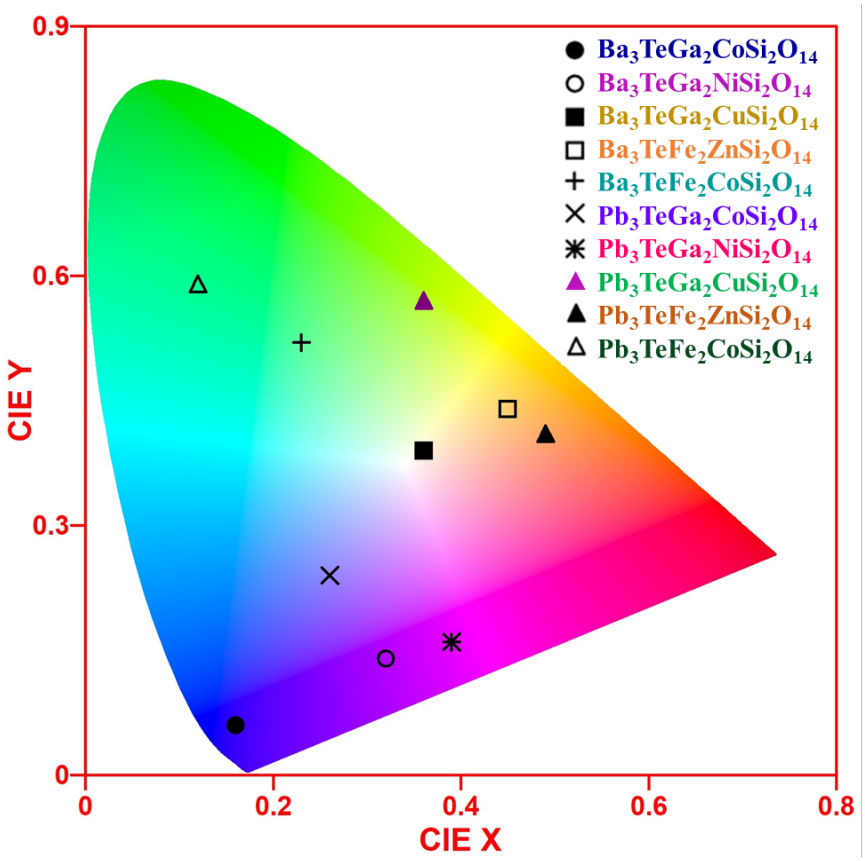

Figure S19. CIE chromaticity diagram for $(Ba/Pb)_3Te(Ga/Fe)_2ZnM^{II}Si_2O_{14}$ (M^{II}=Co, Ni, and Cu) members.

Table S12. Color coordinates for $(Ba/Pb)_3Te(Ga/Fe)_2ZnM^{II}Si_2O_{14}$ (M^{II}=Co, Ni, and Cu) members.

Compound	x	y
$Ba_3TeGa_2CoSi_2O_{14}$	0.16	0.06
$Ba_3TeGa_2NiSi_2O_{14}$	0.33	0.14
$Ba_3TeGa_2CuSi_2O_{14}$	0.36	0.39
$Ba_3TeFe_2ZnSi_2O_{14}$	0.45	0.44
$Ba_3TeFe_2CoSi_2O_{14}$	0.23	0.52
$Pb_3TeGa_2CoSi_2O_{14}$	0.26	0.24
$Pb_3TeGa_2NiSi_2O_{14}$	0.39	0.16
$Pb_3TeGa_2CuSi_2O_{14}$	0.36	0.57
$Pb_3TeFe_2ZnSi_2O_{14}$	0.49	0.41
$Pb_3TeFe_2CoSi_2O_{14}$	0.12	0.59

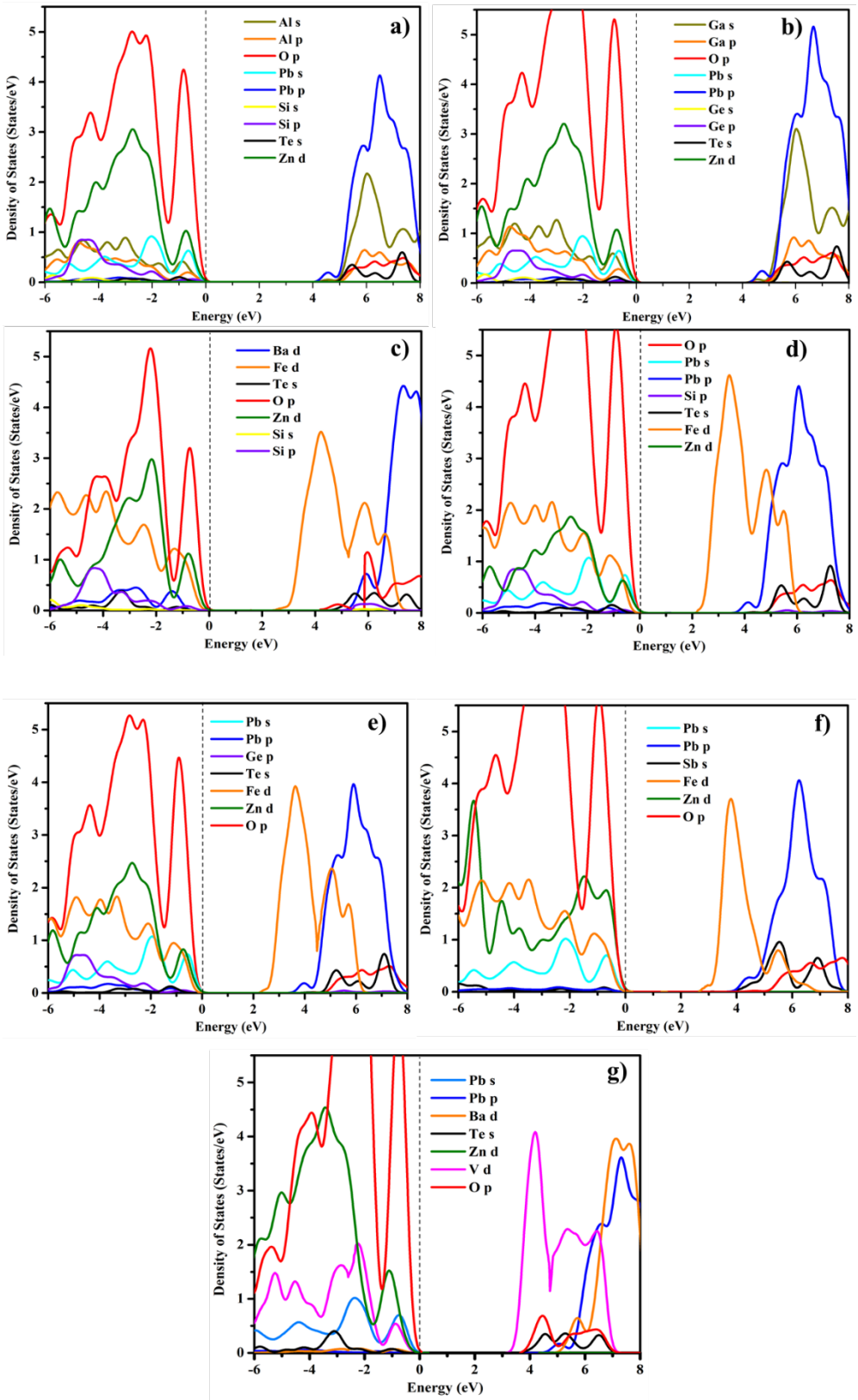

Figure S20. Partial density of states for (a) $Pb_3TeAl_2ZnSi_2O_{14}$, (b) $Pb_3TeGa_2ZnGe_2O_{14}$, (c) $Ba_3TeFe_2ZnSi_2O_{14}$ (d) $Pb_3TeFe_2ZnSi_2O_{14}$ (e) $Pb_3TeFe_2ZnGe_2O_{14}$ (f) $Pb_3SbFeZn_2P_2O_{14}$ (g) $PbBa_2TeZn_3V_2O_{14}$. The Fermi level is set to 0 eV (broken black line).